ChemPlusChem

Research Article
doi.org/10.1002/cplu.202500270

Chemistry Europe
European Chemical Societies Publishing

www.chempluschem.org

Synthesis of New *N,N′*-Diarylureas and Their Theoretical Study as Cannabinoid-1 Receptor Inhibitors

Eirini Tsemperlidou, Nikitas Georgiou, Demeter Tzeli,* Nikolaos Karousis,* and George Varvounis*

A series of new *N,N′*-diarylureas is reported as potential cannabinoid-1 (CB-1) receptor inhibitors. The synthesis of the new *N,N′*-diarylureas is achieved from the reaction of two substituted anilines with the aid of triphosgene. One aniline carries a pyrazol-1-yl or *1H*-1,2,3-triazolyl or *2H*-1,2,3-triazolyl propan-2-one group at position-3, while the other aniline is substituted by fluoro, bromo, methoxy, cyano, morpholino, or 4-methyl-2-nitro groups. All new compounds are investigated through density functional theory calculations, molecular docking, and molecular dynamics simulations, showing a strong ability to bind to the orthosteric pocket of the CB-1 receptor and to the allosteric position when CB1 is in complex with agonist AM841. The binding is comparable to that of the well-known CB-1 inhibitor PSNBAM-1. Especially, 1-{3-[2-(1*H*-pyrazol-1-yl)acetyl]phenyl}-3-(4-methyl-3-nitrophenyl)urea presents better theoretical results than PSNBAM-1.

1. Introduction

Cannabinoid type-1 (CB1) receptor is a G-coupled protein receptor, abundantly present in brain tissue and neuronal cells, and is responsible for inhibiting the release of neurotransmitters in the central nervous system, influencing processes such as memory, learning, motor functions, and pain transmission.[1] CB1 has been identified in several disorders including drug addiction,[2] gastrointestinal diseases,[3] inflammation,[4] multiple sclerosis,[5] obesity,[6] osteoporosis,[7] inflammatory pain,[8] psychosis,[9] schizophrenia,[10] and smoking,[11] and is therefore considered a promising target for their treatment. In addition to the brain, the CB1 receptor also functions, though to a lesser extent, in the liver, adipose tissue, vascular and cardiac tissues, as well as in reproductive tissues and bone. First-generation CB1 receptor antagonists/inverse agonists (i.e., rimonabant) were developed and used in the treatment of obesity; however, they were quickly withdrawn from the European Union market and denied approval by the US Food and Drug Administration because of their association with gastrointestinal and mainly psychobehavioral adverse effects, leading to unacceptable benefit-to-risk profiles.[12] Since 2005 ongoing research has suggested that allosteric modulators of the CB1 receptor could serve as an alternative method to regulate the CB1 receptor for therapeutic purposes.[13] In this context, the *N,N′*-diarylurea derivative PSNCBAM-1 (**Figure 1**) has played a key role in this research by presenting a two-fold activity: First, as a positive allosteric modulator regarding the binding affinity of orthosteric ligands and at the same time as a negative allosteric modulator regarding the functional activity of orthosteric ligands.[14] *N,N′*-diarylurea is a key pharmacophore in anticancer drugs like Sorafenib, an oral multikinase inhibitor for treating advanced renal cell carcinoma. This intense area of research has led to the publication of several review articles.[15] *N,N′*-diarylurea A (Figure 1) was the first $P2Y_1$ antagonist to show a strong oral antithrombotic effect with mild bleeding risk in rat thrombosis and hemostasis models.[16] Other important pharmaceutical applications of *N,N′*-diarylureas include antimicrobial properties that are particularly effective against schistosomiasis,[17] malaria,[18] and tuberculosis infections.[19]

The first synthetic methods for producing both symmetrical and unsymmetrical *N,N′*-diarylureas appeared back in sixties and primarily involved phosgenation of aryl amines. Another method for the synthesis of symmetrical *N,N′*-diarylureas is fusion of urea with excess aryl amines at 120–190 °C. Over the next two decades, several other methods for synthesizing (un)symmetrical

E. Tsemperlidou, N. Karousis, G. Varvounis
Laboratory of Organic Chemistry
Department of Chemistry
University of Ioannina
Ioannina 45110, Greece
E-mail: nkarousis@uoi.gr
gvarvoun@uoi.gr

N. Georgiou
Laboratory of Organic Chemistry
Department of Chemistry
National and Kapodistrian University of Athens, Panepistimioupolis Zografou
Athens 15784, Greece

D. Tzeli
Laboratory of Physical Chemistry
Department of Chemistry
National and Kapodistrian University of Athens, Panepistimioupolis Zografou
Athens 15784, Greece
E-mail: tzeli@chem.uoa.gr

D. Tzeli
Theoretical and Physical Chemistry Institute
National Hellenic Research Foundation
48 Vassileos Constantinou Ave., Athens 11635, Greece

Supporting information for this article is available on the WWW under https://doi.org/10.1002/cplu.202500270

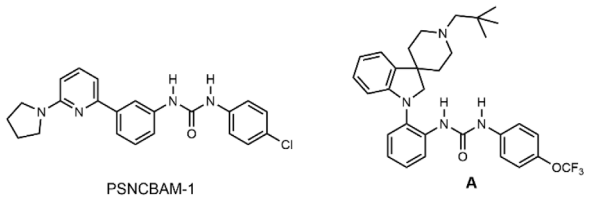

Figure 1. Biologically active *N,N′*-diarylureas.

N,N′-diarylureas appeared in the literature. These methods include carbonylation of aryl amines, either under 100 atm CO at 100–200 °C in the presence of $Mn_2(CO)_{10}$ or using nitroarenes with a catalytic amount of $PtCl_2(Ph_3P)_2$,[20] as well as oxidative carbonylation of nitroarenes and corresponding aryl amine in $BMImBF_4$ with elemental sulfur under 3.0 MPa of CO.[21] A comprehensive review article dealing only with the synthesis of unsymmetrical *N,N′*-diarylureas appeared in 2007.[22] After the introduction of crystalline triphosgene as a safe alternative to phosgene, triphosgene, and diisopropylamine, combined with the sequential addition of two different aryl amines to produce unsymmetrical *N,N′*-diarylureas.[23] In fewer cases, *N,N′*-carbonyldiimidazole (CDI)[24] can also be used. *N*-Aryl formamides react efficiently with aryl amines and a catalytic amount of $RuCl_2(PPh)_3$ to yield a variety of symmetrical *N,N′*-diarylureas.[25] The Pd-catalyzed arylation of urea or phenylurea, in the presence of Pd_2dba_3, Xantphos, and aryl bromides, produces symmetrical and unsymmetrical *N,N′*-diarylureas, respectively.[26] Two comparable coupling reactions with phenylurea, aryl iodides, and CuI as catalyst use either *N,N′*-dibenzylethylenediamine and KF/Al_2O_3[27] or *N,N′*-dimethylethylenediamine and K_3PO_4,[28] to yield (un)symmetrical *N,N′*-diarylureas. A variety of monoaryl ureas are synthesized in one pot by crosscoupling of benzyl urea with aryl chlorides and $Pd(OAc)_2$ as catalyst, followed by hydrogenolysis. A second arylation of monoaryl ureas with aryl chlorides, under similar conditions, yields unsymmetrical *N,N′*-diarylureas.[29]

Microwave irradiation of aryl amines and ethyl acetoacetate, without catalysts and under solvent-free conditions, yields symmetrical *N,N′*-diarylureas, as does the same method but using diphenyl ether as solvent.[30] Aryl amines react with phenyl chloroformate to yield phenyl carbamates, which further react with aryl amines to afford unsymmetrical *N,N′*-diarylureas.[31]

Aryl isocyanates, which are now commercially available and simple to synthesize, are attractive starting materials for producing *N,N′*-diarylureas. A significant number of (un)symmetrical *N,N′*-diarylureas have been synthesized from aryl isocyanates and aryl amines for the purpose of biological evaluation.[19,32,31a] *N*-acylbenzotriazoles (ArCOBt), derived by the reaction of corresponding aromatic carboxylic acids with benzotriazole in $SOCl_2$, are induced by NaN_3 in tetrahydrofuran (THF):water (85:15) to undergo the Curtius rearrangement and give intermediate aryl isocyanates that slowly hydrolyze to aryl carbamic acids and decarboxylate to intermediate aryl amines, finally to combine with aryl isocyanates to generate symmetrical *N,N′*-diarylureas.[33] Using a similar method, *N*-acylbenzotriazoles react with various aryl amines in the presence of $TMSN_3$ and Et_3N to afford (un)symmetrical *N,N′*-diarylureas.[34]

It was recently reported that unsymmetrical *N,N′*-diarylureas can be synthesized utilizing 3-aryl-substituted dioxazolones as precursors of aryl isocyanates, along with aryl amines, in methanol-containing sodium acetate.[35] Recently, Audisio and co-workers[36] reported a continuous flow synthetic process for producing unsymmetrical *N,N′*-diarylureas, which involved a Staudinger/aza-Wittig reaction sequence utilizing aryl azides, aryl amines, and methyldiphenylphosphine. *N,N′*-diarylureas of medical importance, whose chemical and biological properties play a significant role in drug design and discovery, are presented by Ghosh and Brindisi.[37]

Herein, we present the synthesis of 17 new diaryl ureas. The main structural differences of diaryl ureas with respect to the known allosteric CB1 inhibitor PSNCBAM-1 are represented by the replacement of the pyridine and pyrrolidine rings with a pyrazolo- or triazolo-ring and a methylenecarbonyl spacer. In an analogy with PSNCBAM-1, diaryl ureas are characterized by a chlorine substituent in the peripheral aromatic ring at the *para*-position, while a series of other substituents, including, fluoro, bromo, methoxy, cyano, morpholino, and 4-methyl-2-nitro, were also used. All the new compounds were investigated through theoretical studies with the aid of density functional theory (DFT) calculations, molecular docking, and molecular dynamics simulations.

2. Results and Discussion

2.1. Chemistry

The general synthesis of pyrazolo-based *N,N′*-diarylureas is illustrated in **Figure 2**. Bromination of the commercially available 3-nitroacetophenone **1** took place in chloroform, and after treatment with cold ethanol, 2-bromo-1-(3-nitrophenyl)ethanone **2** was obtained in 95% yield. Subsequently, substitution of the bromine atom of **2** by 1*H*-pyrazole in anhydrous *N,N*-dimethylformamide, in the presence of potassium carbonate as a base, led to 1-(3-nitrophenyl)-2-(1H-pyrazol-1-yl)ethanone **3** as a yellow amorphous solid, in 74% yield. It should be mentioned that a total of 10 variable reaction conditions were examined at this step, in terms of different bases, reaction time, and temperature, with the aim of achieving the above-mentioned optimum final yield for **3**. The reduction reaction of **3** to the corresponding amino-derivative **4** was carried out with the aid of iron sulfate heptahydrate in a mixture of boiling aqueous ammonia (25% v/v) and ethanol for 2 h. 1-(3-Aminophenyl)-2-(1H-pyrazol-1-yl)ethan-1-one **4** was obtained in the form of a brown-yellow amorphous solid, in 96% yield. Finally, pyrazoloaniline derivative **4** was reacted with 1/3 equivalent of triphosgene and 2 equivalents of anhydrous triethylamine, in anhydrous tetrahydrofuran at 0 °C for 2 h, to produce the isocyanate intermediate **5**, which, without isolation, was reacted with 2 equivalents of the appropriate aniline, at room temperature for 1.5 to 60 h to form the corresponding *N,N′*-diaryl ureas **6a** to **6i**, in 15%–86% yield.

The synthetic pathway for triazolo-based *N,N′*-diarylurea analogues is presented in **Figure 3**. The reaction between 2-bromo-1-(3-nitrophenyl)ethanone **2** and 1*H*-1,2,3-triazole took place in

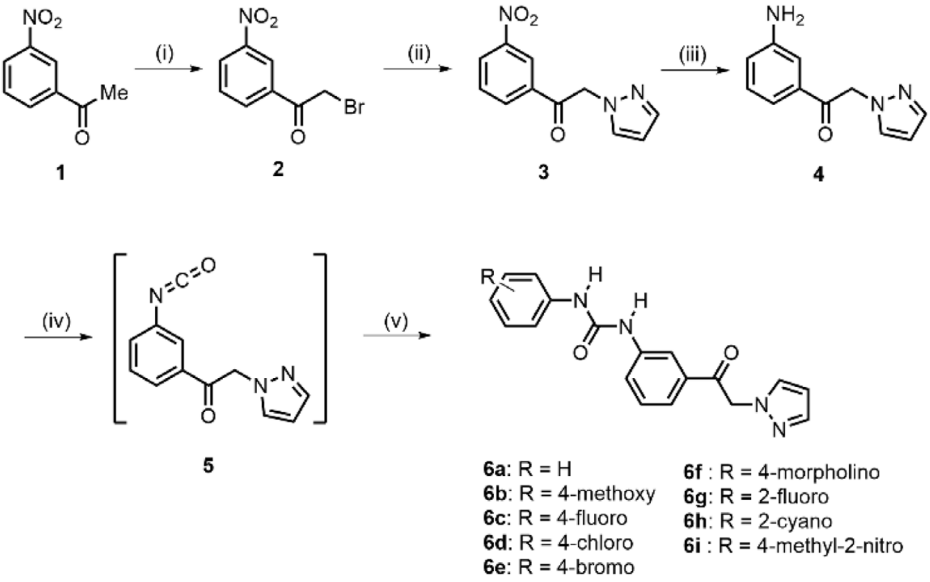

Figure 2. Schematic representation for the synthesis of diarylurea derivatives **6a–6i**. i) Br_2, $CHCl_3$, 0 °C, 1.5 h; ii) 1*H*-pyrazole, dry DMF, 0 °C, then K_2CO_3, H_2O, r.t.; iii) $FeSO_4.7H_2O$, 25% NH_4OH, 95% EtOH, reflux, 2 h; iv) $(Cl_3CO)_2CO$ (1/3 equiv.), dry THF, dry Et_3N (2 equiv.), 0 °C, 2 h; v) $RC_6H_4NH_2$ (**R**=H, 4-MeO-, 4-F-, 4-Cl-, 4-Br-, 4-morpholino-, 2-F-, 2-CN-, 4-methyl-2-nitro-) (2 equiv.), dry THF, 1.5–60 h, r.t.

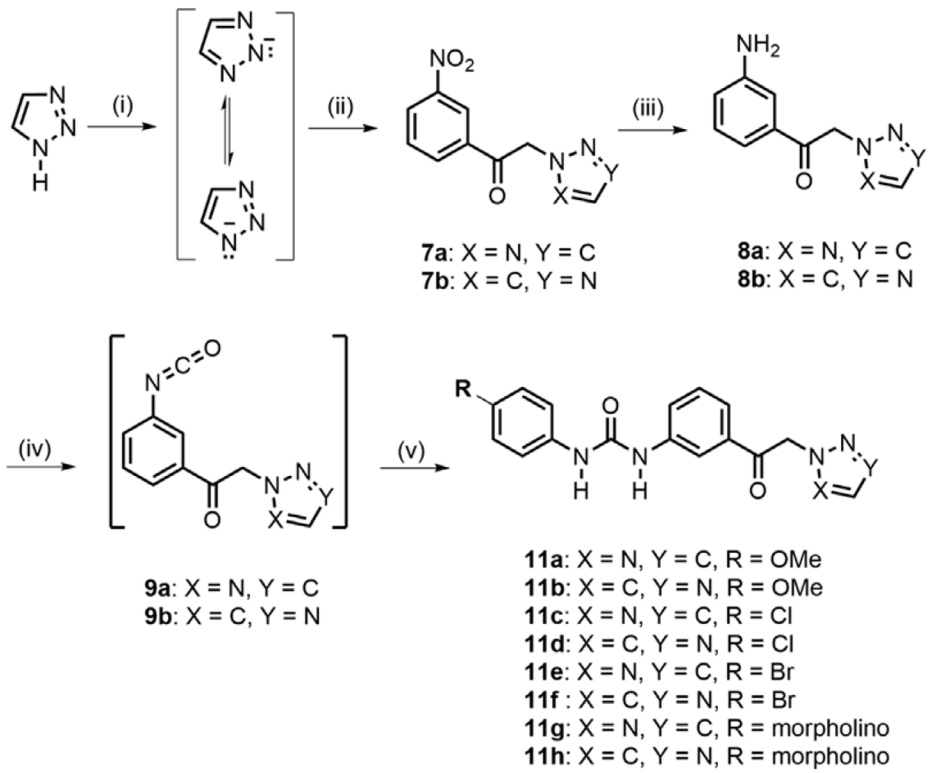

Figure 3. Schematic representation for the synthesis of diarylurea derivatives **11a–11h**. i) N,N-Diisopropylethylamine, dry MeCN, r.t. 0.5 h ii) **2**, r.t. 18 h; iii) for **7a**: $FeSO_4.7H_2O$, 25% NH_4OH, *i*-PrOH, reflux, 2 h; for **7b**: $SnCl_2.2H_2O$ MeOH, 60 °C, 3 h iv) $(Cl_3CO)_2CO$ (1/3 equiv.), dry THF, dry Et_3N (2 equiv.), 0 °C, 2 h; (v) $RC_6H_4NH_2$ **10** (R = MeO-, Cl-, Br-, morpholino-), dry THF, 48 h, r.t.

the presence of triethylamine in acetonitrile at room temperature and resulted in a mixture of 1-(3-nitrophenyl)-2-(1H-1,2,3-triazol-1-yl) ethan-1-one **7a** and 1-(3-nitrophenyl)-2-(2H-1,2,3-triazol-1-yl) ethan-1-one **7b**, in a ratio of 2.3:1. The separation of the two products of this reaction is complex due to their poor solubility in both nonpolar and polar solvents. In this context the isolation of **7b** was achieved through continuous dispersion-precipitation cycles in ethyl acetate to remove **7a** as well as the less polar

reaction byproducts, which are soluble in ethyl acetate. Subsequently, purification of the resulting filtrate by medium-pressure column chromatography and recrystallization of the isolated solid with ethyl acetate and hexane led to **7a** as needle-like yellow crystals, while **7b** was obtained as an amorphous white solid.

The distinction between the two isomeric products 2H-1,2,3-triazole **7a** and 1*H*-1,2,3-triazole **7b** is easily accomplished by ^{1}H NMR spectroscopy (Figures S35 and S37). Both spectra present two singlet peaks at 6.38 and 6.33 ppm, which are designated to the methylene group protons of **7a** and **7b**, respectively. Another set of common peaks in the spectra of the 1*H*- and 2*H*-isomers relates to the aromatic protons H-2′, H-6′, and H-4′ of the benzene ring. The H-2′ of the phenyl ring of **7a** and **7b** isomers gives a triplet peak at 8.73 and 8.77 ppm, respectively, with a similar $J = 2.0$ Hz. A *doublet of triplets* (*dt*) at 8.45 ppm ($J = 7.8$, 1.7 Hz) and 8.49 ppm ($J = 7.8$, 1.3 Hz ppm) is assigned for H-6′, and a *doublet of doublets of doublets* (*ddd*) at 8.56 ppm ($J = 8.2$, 2.4, 1.0) and 8.54 ppm ($J = 8.2$, 2.3, 1.0 Hz) is assigned for H-4′, for **7a** and **7b**, respectively. The main difference in the spectra of the two isomers lies in the triazole protons H-4 and H-5. In the case of the symmetric triazole ring **7a**, protons H-4 and H-5 are chemically equivalent due to being in the same chemical environment, resulting in a triplet peak at 7.89 ppm, which also comprises H-5′ of the aromatic phenyl ring. In the case of isomer **7b**, the hydrogen bonding interaction between the carbonyl oxygen atom and the adjacent H-5 deshields the signal of the latter at 8.11. On the other hand, H-4 of the triazole ring in **7b** is shielded, giving a signal at 7.82 ppm, while H-5′ of the phenyl ring of **7b** appears as a triplet at 7.92 ppm.

The synthesis of the two triazoloethanone isomers, **7a** and **7b**, was followed by their reduction to the corresponding amino compounds, **8a** and **8b**, respectively. The reduction of isomer **7a** proceeded smoothly using iron sulfate heptahydrate and 25% v/v aqueous ammonia in isopropanol solvent. After boiling the solution for 2 h and removing the formed iron oxides, the desired amino-derivative **8a** was obtained as a brown-yellow amorphous solid, in 93% yield. In contrast, the reduction of amino derivative **7b** proved more challenging in terms of finding suitable chemical conditions. In addition to iron sulfate heptahydrate, several catalysts and reducing procedures were tested, including catalytic hydrogenation in the presence of platinum dioxide catalyst (10%, Adams catalyst) or with palladium on carbon catalyst. However, none of these gave any product. The reduction of **7b** took place in the presence of tin chloride dihydrate according to the method of Bellamy.[38] A solution of nitro compound **7b** in methanol was heated gently at 55–60 °C for 2 h, resulting in the production of the hydrochloride salt of the amine, as the reaction environment was strongly acidic (pH = 1). Subsequent basification of the solution (pH = 8) resulted in the formation of amino-derivative **8b**, which is obtained as a yellow amorphous

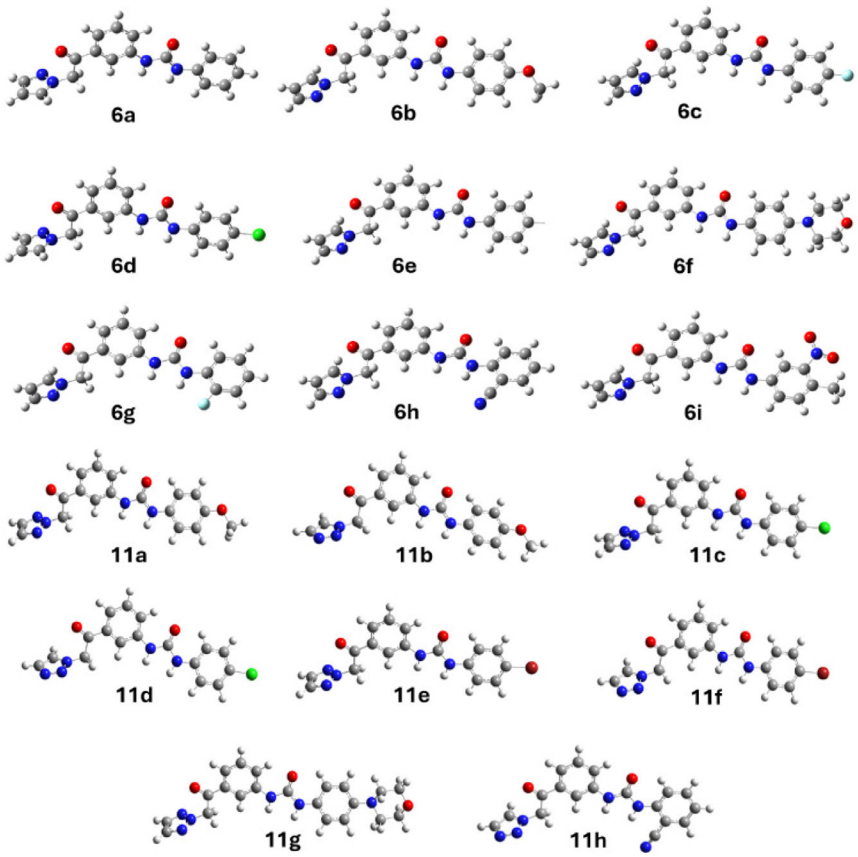

Figure 4. Calculated minima structures of new *N,N′*-diarylureas **6a–i** and **11a–h** at the B3LYP/6-311+g(d,p) methodology in THF solvent. (Atoms C = grey balls, H = white, O = red and N = blue).

solid, in 87% yield. In the final step of the synthetic route, each of amino derivatives **8a** and **8b** reacted with 1/3 equivalent of triphosgene and 2 equivalents of anhydrous triethylamine in anhydrous tetrahydrofuran at 0 °C for 2 h, followed by the addition of 2 equivalents of the appropriate aniline **10** to form the corresponding *N,N′*-diaryl ureas **11a–h**, respectively.

2.2. Theoretical Studies

The aims of the theoretical calculations are: 1) to investigate the binding of the new *N,N′*-diarylureas **6a–i** and **11a–h** in CB1 and 2) to correlate the molecular structure of **6a–i** and **11a–h** with their reactivity to interact with their binding in the CB1. Specifically, the binding of **6a–i** and **11a–h** in the allosteric position of CB1 is investigated when CB1 is a complex with agonist AM841, and it is compared with the binding of the well-known CB-1 inhibitor PSNBAM-1 via molecular docking. Furthermore, the binding of these new *N,N′*-diarylureas and of PSNBAM-1 in the orthosteric position of CB-1 is also studied via molecular docking and molecular dynamics. Finally, the molecular structure of **6a–i** and **11a–h** and their reactivity tendency are investigated via DFT calculations.

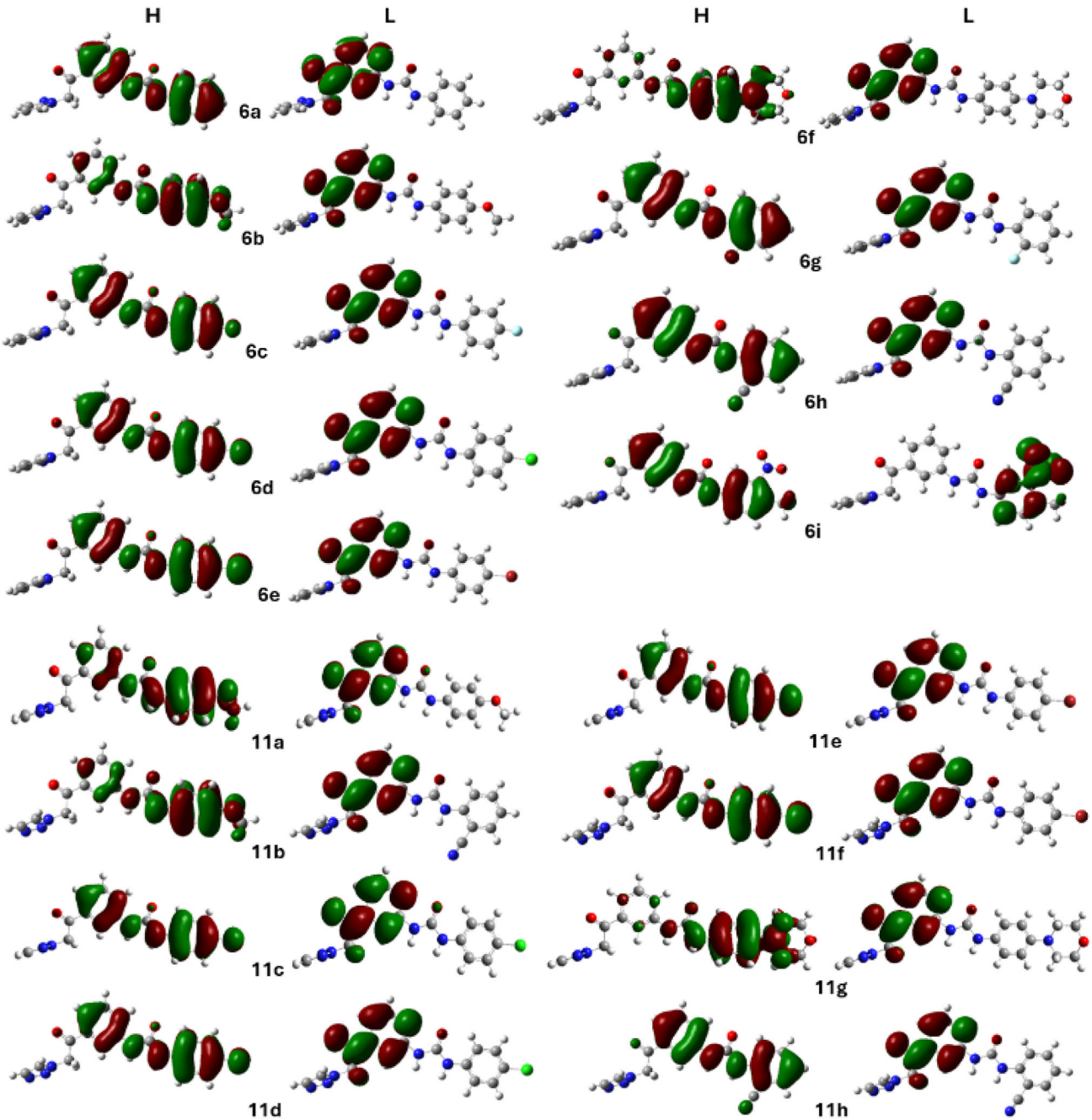

Figure 5. Calculated minima structures of new *N,N′*-diarylureas **6a–i** and **11a–h** at the B3LYP/6-311+g(d,p) methodology in THF solvent. (Atoms C = grey balls, H = white, O = red and N = blue).

2.2.1. DFT Calculations

At first, a conformational analysis was carried out to find the lowest-energy structures of the *N*,*N*′-diarylureas. The calculated structures at the B3LYP/6-311+g(d,p)[39,40] methodology in THF solvent using the polarizable continuum model (PCM model)[41] are depicted in **Figure 4**. The DFT methodology has been shown to predict well the geometries and energetics,[42,43] while it has been shown that the PCM model describes well the solvent effects.[44] Further details on the methodology are given in SI. Their geometry of the calculated structures is given in Table S1 of the Supporting Information. All DFT calculations have been carried out via the Gaussian16 program.[45]

The highest occupied molecular orbitals (HOMO) and lowest unoccupied molecular orbitals (LUMO) of the diarylureas **6a–i** and **11a–h** are depicted in **Figure 5**, and their energy is given in Table S2 of Supporting Information. The energy difference between the HOMO and LUMO orbitals may be indicative of their reactivity, especially when the molecules are similar and only some of their peripheral groups differ.[46] Thus, a small HOMO–LUMO difference (ΔE_{HL}) can be related to a large reactivity, while large ΔE_{HL} values with a small reactivity.[47] It should be noted that the energy difference between the HOMO and LUMO orbitals is dependent on the DFT methods;[48] however, within the same methodology, the ΔE_{HL} values for similar molecules differing only in their distant groups can give some trends regarding their reactivity. In general, the use of ΔE_{HL} values as a reactivity indicator should be taken with cautious; however, the present studied compounds is a case where they can be used. The B3LYP/6-311 + g(d,p) in THF solvent HOMO–LUMO energy difference is given in **Table 1**. It is found that the order of the *N*,*N*′-diarylureas **6a–6i** and **11a–11 h** starting from the molecule with the smallest H-L energy difference to the largest one is **11g** < **6f** < **6i** < **11b** < **11a** < **6b** < **6a** < **11f** < **11d** < **11e** < **11c** < **6c** < **6e** < **6d** < **6g** < **11h** < **6h**. Thus, the three *N*,*N*′-diarylureas **11g**, **6f,** and **6i** present increased reactivity and may interact better with the CB1 receptor.

The frontier molecular orbitals for each compound are shown in Figure 5. In all cases, the H to L excitation corresponds to a charge transfer process. In all compounds, the electron density of the HOMO orbitals is localized at the two aromatic rings and the urea groups, apart from the **6f** and **11g**, where their HOMO orbital is localized at the urea and the right aromatic group with the 4-morpholino group. On the contrary, in all compounds, the electron density of the LUMO orbitals is localized only in the center aromatic ring, except for **6i**, where it is located at the Ph-NO_2 group. So, the charge transfer is from the right aromatic ring and urea group to the center aromatic group. In the case of the **6i** compound, the charge transfer is from the central aromatic ring and the carbonyl groups to the Ph-NO_2 group. However, in the cases of the **6f** and **11g**, instead of an H → L charge transfer process, an electron transfer has occurred; that is, their HOMO and LUMO orbitals do not have electron density at the same common groups. Thus, to sum up, the **11g**, **6f,** and **6i** *N*,*N*′-diarylureas present some differences in the electron density of their HOMO and LUMO orbitals with respect to the remaining *N*,*N*′-diarylureas.

2.2.2. Molecular Docking

Induced fit docking was employed to investigate potential binding interactions in the allosteric blind position of the CB-1 receptor (PDB ID: 5XR8).[49] The in silico studies were conducted using the Protein Preparation Wizard in the Schrödinger Suite to process the crystal structures. At first, all the compounds underwent energy minimization using MacroModel[50] and DFT calculations. Conformer analysis ensured the identification of stable low-energy geometries through DFT, while molecular mechanics provided further refinement, balancing accuracy and computational efficiency. LigPrep was utilized to generate 3D models, accounting for stereochemistry, and the "add metal binding states" option was applied to optimize ligand binding. Geometry optimization in MacroModel preserved chirality, with the OPLS2005 force field employed for minimization while considering protonation states at physiological pH. Chemically accurate 3D models were generated using the Hammett and Taft methods alongside an ionization tool. Ligand structures were further minimized in a water environment using the OPLS2005[51] force field. To explore the most stable conformations, a mixed-torsional/low-sampling conformational search was performed, and the lowest-energy conformer was selected for docking studies. The induced fit docking (IFD) approach in the Schrödinger Suite was utilized for docking, with the ligand being docked in five energetically favorable conformations obtained from MacroModel. Prior to docking,

Table 1. Energy difference of the HOMO–LUMO orbitals, ΔE_{HL} (eV), of the diary ureas **6a–6i** and **11a–11h** at the B3LYP/6-311 + g(d,p) methodology in THF solvent using the PCM model.

a/a	Diaryl urea	ΔE_{HL}	a/a	Diaryl urea	ΔE_{HL}
1	**6a**	3.896	10	**11a**	3.648
2	**6b**	3.708	11	**11b**	3.577
3	**6c**	4.011	12	**11c**	3.983
4	**6d**	4.022	13	**11d**	3.944
5	**6e**	4.017	14	**11e**	3.976
6	**6f**	3.315	15	**11f**	3.938
7	**6g**	4.103	16	**11g**	3.253
8	**6h**	4.256	17	**11h**	4.186
9	**6i**	3.537	–	–	–

Table 2. Molecular docking results for 17*N*,*N*′-diarylureas and of the known inhibitor PSNCBAM-1 in allosteric position of the receptor CB1 complex with the agonist AM841.

a/a	Diaryl urea	Docking score (kcal mol^{-1})	a/a	Diaryl urea	Docking score (kcal mol^{-1})
1	**6a**	−4.60	10	**11a**	−4.05
2	**6b**	−5.03	11	**11b**	−4.95
3	**6c**	−5.16	12	**11c**	−4.60
4	**6d**	−5.80	13	**11d**	−5.16
5	**6e**	−5.61	14	**11e**	−6.17
6	**6f**	−4.85	15	**11f**	−4.19
7	**6g**	−5.19	16	**11g**	−3.38
8	**6h**	−4.44	17	**11h**	−4.39
9	**6i**	−4.93	18	PSNCBAM-1	−4.85

protein preparation involved constrained refinement, which included automatic side-chain trimming based on B-factor analysis and Prime-based side-chain optimization. The Glide/XP docking tool was used, with an active-site dielectric constant set to 80, and crystallographic water molecules were retained throughout the docking process.

2.2.3. Allosteric Site

For all *N,N′*-diarylureas **6a–i** and **11a–h** and the known inhibitor PSNCBAM-1, blind molecular docking calculations were performed to find an allosteric position to bind in the CB1-AM841 complex. AM841 is an orthosteric agonist, meaning it binds directly to the orthosteric site of CB1, which is the primary binding site. It was found that all *N,N′*-diarylureas and the known inhibitor PSNCBAM-1 prefer to bind to the same allosteric position in CB1. Numerous conformations were generated; the results of the most favorable values are shown in **Table 2**.

The strongest docking scores are obtained for the compounds **11e** (-6.17 kcal mol^{-1}), **6d** (-5.88 kcal mol^{-1}), and **6e** (-5.61 kcal mol^{-1}), see Table 2. For the known inhibitor PSNCBAM-1, the docking score is -4.85 kcal mol^{-1}. Note that 10 out of the 17 studied *N,N′*-diarylureas, that is, **11e, 6d, 6e, 6g, 11d, 6c, 6b, 11b, 6i,** and **6f**, bind stronger than the known inhibitor PSNCBAM-1 or similar

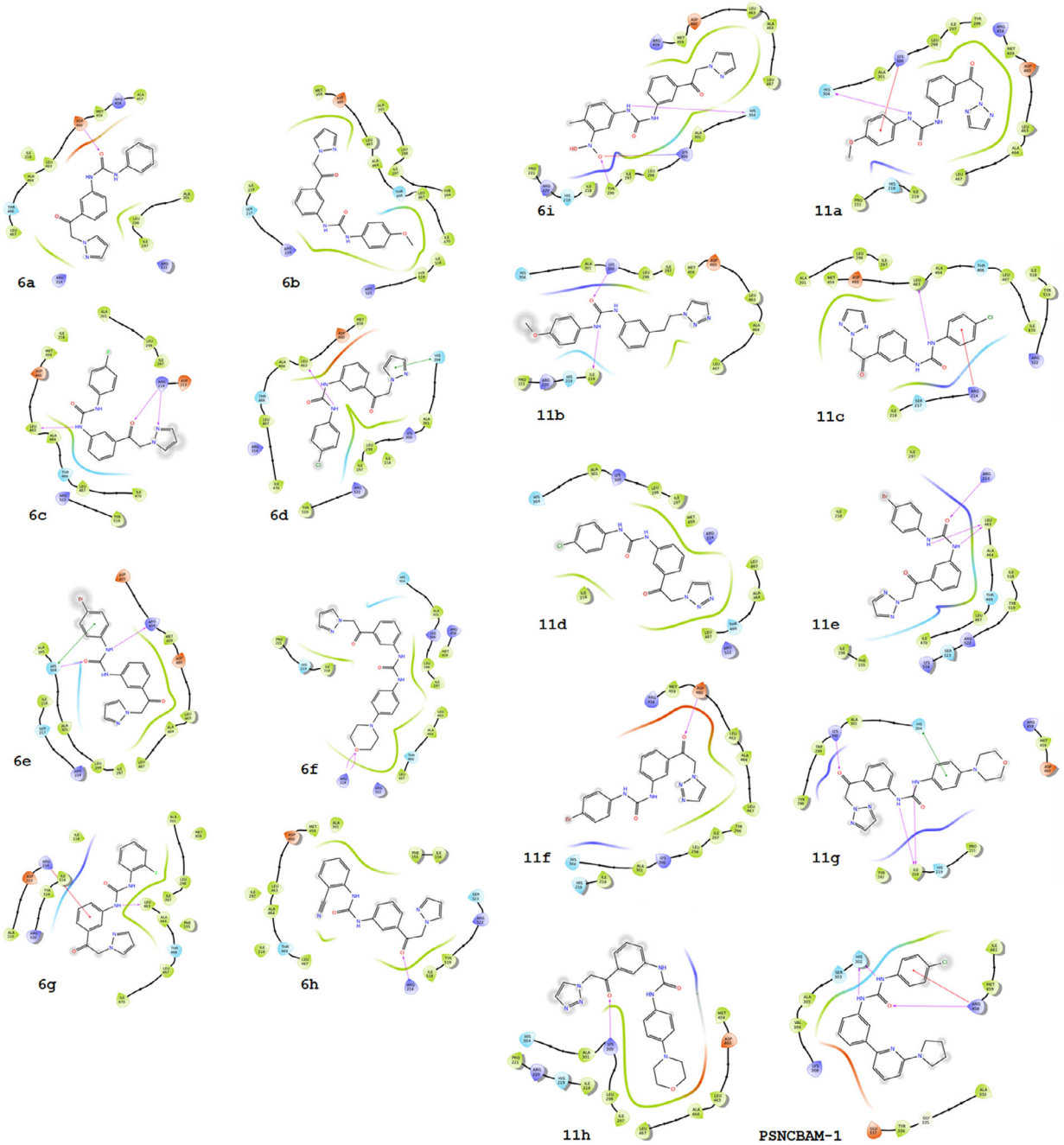

Figure 6. Binding interactions of *N,N′*-diarylureas **6a–i**, **11a–h** and inhibitor PSNCBAM-1 with the allosteric site of the CB1 receptor in complex with the agonist AM841.

with it. Thus, the above 10 compounds have the potential to be used successfully as allosteric CB-1 receptor inhibitors.

The interactions of each diarylurea with the amino acids of the allosteric site are shown in **Figure 6**. As can be seen from Figure 6, all compounds bind to the same pocket in the enzyme. They are located next to the same amino acids, and they bind in an allosteric position. Selected interactions are given in **Table 3**. In detail, compound **6a** forms one hydrogen bond with ASP460, and compound **6c** forms three hydrogen bonds with ARG214 and LEU463. Moreover, compound **6d** forms one hydrogen bond with LEU463 and one π–π interaction with HIS304, while compound **6e** forms one hydrogen bond with ARG458 and one π–π interaction with HIS304. Also, compound **6g** forms one hydrogen bond with LEU463 and one cation–π interaction with ARG214, compound **6h** forms one hydrogen bond with ARG214, while compound **6i** forms two hydrogen bonds with HIS304 and TYR296.

2.2.4. Orthosteric Site

The docking scores of compounds **1a–6i** and **11a–11h** at the orthosteric pocket of CB1, that is, in the primary binding site where the agonist AM841 binds, have been calculated; see Supporting Information, Table S3. The docking scores are higher than the corresponding values at the allosteric site, as is expected. The stronger values are obtained for the **6f**, **6i**, and **11g** compounds, which present the same strong binding score with the known inhibitor PSNCBAM-1, thus indicating that they are the best candidates as inhibitors to CB1 among the present calculated *N*,*N*′-diarylureas. Furthermore, it seems that **6i** is a better inhibitor than the PSNCBAM-1.

The interactions of studied diarylureas in the orthosteric binding site of CB1 are shown in **Table 4**. Specifically, diarylurea **6i** forms one hydrogen bond with PHE174 amino acid. Furthermore, diarylurea **6f** forms two π–π interactions with TRP279 and two hydrogen bonds with PHE117. Also, diarylurea **11g** forms 5 π–π interactions with TRP279, PHE268, PHE501, and PHE174. Diaryl-urea **6b** forms two π–π interactions with PHE279 and PHE189, and diarylurea **6c** forms one π–π interaction with TRP275. The interactions are similar for each diarylurea.

It is interesting that the three compounds, **6f**, **6i**, and **11g**, that present the strongest binding values in the main/primary binding site of the CB1 present an increased reactivity trend, as has been shown from the DFT calculations. On the contrary, for the allosteric binding, where the docking score is smaller than the scores in the orthosteric site, the favored compounds, that is, compounds forming the strongest values for the allosteric site, do not follow the DFT reactivity trend. This may occur because, when a ligand binds tightly, the binding interaction is often specific and directional (e.g., involving charge transfer, hydrogen bonding, or π–π stacking). In these cases, a smaller HOMO–LUMO gap, that is, a more reactive molecule, often is correlated with a greater ability to donate (HOMO) or accept (LUMO) electrons, a better stabilization of the interaction via orbital overlap (especially in metal–ligand or π-systems), and enhanced charge transfer interactions with the receptor. Therefore, in strong binders, the binding interaction may rely heavily on electronic reactivity, and thus the HOMO–LUMO difference is crucial and aligns with the docking score. On the contrary, in weak binding, other factors or randomness dominate; for instance, the ligand may not be properly oriented in the binding site, steric issues, or poor docking poses obscure electronic effects. In cases of medium binding interaction, the electronic reactivity (HOMO–LUMO) may no longer drive the docking outcome, so no meaningful correlation is observed. Thus, in the allosteric site, where the drugs are less bound than in the orthosteric site, their reactivity is less important for the binding.

Table 3. Interactions of *N*,*N*′-diarylureas with the allosteric site of the CB1 receptor in complex with the agonist AM841.

a/a	Diarylurea	Hydrogen bonding	π–π interaction
1	**6a**	Asp460	–
2	**6c**	Leu463, Arg214(2)	–
3	**6d**	Leu463	His304
4	**6e**	His304, Arg458	His304
5	**6f**	Arg214(2)	–
6	**6g**	Leu463	Arg214
7	**6h**	Arg214	–
8	**6i**	His304, Lys300, Tyr296	–
9	**11a**	His304	Lys300
10	**11b**	Ile218, Lys300	–
11	**11c**	Leu463	Arg214
12	**11e**	Leu463(2), Arg214	–
13	**11f**	Asp460	–
14	**11g**	Ile218(2), Lys300	His304
15	**11h**	Lys300	–
16	PSNCBAM-1	His302(2), Arg458	Arg458

Table 4. Interactions of *N*,*N*′-diarylureas with the orthosteric site of CB1.

a/a	Diarylurea	Hydrogen bonding	π–π interaction
1	**6b**	–	PHE279, PHE189
2	**6c**	–	TYR275
3	**6f**	PHE177	TRP279
4	**6g**	PHE174	PHE268
5	**6h**	PHE177	PHE177
6	**6i**	PHE174	–
7	**11a**	PHE501	PHE170
8	**11b**	–	PHE268
9	**11c**	–	TRP279
10	**11d**	–	TRP475, PHE501, PHE268
11	**11e**	SER505	–
12	**11f**	–	TYR275
13	**11g**	–	PHE174, PHE268, PHE501, TRP279
14	**11h**	PHE174	–
15	PSNCBAM-1	PHE174	–

2.2.5. Molecular Dynamics Simulations

Molecular dynamics (MD) was carried out for the *N*,*N*′-diarylureas that bind strongly to the active center to investigate if the

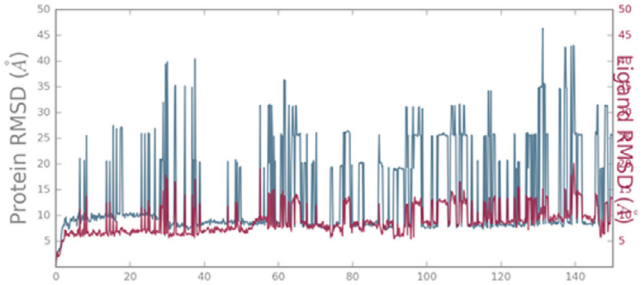

Figure 7. RMSD value for the protein (CB1) (depicted in green) and the diarylurea **11e**.

diarylurea remains stable in the active center of the protein (primary binding site). The root-mean-square deviation (RMSD) for both protein and diarylurea was calculated during the MD, which is a measure of the average distance between atoms of superimposed protein structures and diarylurea structures, respectively; see Figure S6 of SI.

Specifically, the binding affinity of compounds **6f**, **6i**, and **11g** during the time evolution of 200 ns was investigated. It was found that when diarylurea **6f** is docked, the protein undergoes significant conformational changes, or there are regions in the protein that are very flexible during the simulation, while **6f** remains bound, maintaining its binding orientation, experiencing only slight positional or orientational shifts over time. As regards **6i**, the protein undergoes significant conformational changes, or there are regions in the protein that are very flexible during the simulation, while **6i** also presents fluctuations even though they seem more stable in comparison to protein. Finally, for diarylurea **11g**, the protein maintains structural integrity while **11g** undergoes substantial movements or conformational changes within the binding site; see SI.

Regarding the binding affinity of compound **11e**, which presents the largest docking score at the allosteric site of CB-1, the time evolution of 200 ns was investigated; see **Figure 7**. It was found that the protein's RMSD fluctuates significantly, indicating substantial conformational changes, while the ligand RMSD remains relatively stable with smaller variations, suggesting that the ligand maintains a consistent binding pose throughout the simulation. Thus, **11e** remains bonded in the allosteric position.

3. Conclusion

In this study, a series of new pyrazolo- and triazolo-based diaryl ureas were successfully synthesized with the goal of obtaining novel selective CB1 receptor antagonists. The role of the *para*-substituents of the phenyl group in CB1 receptor antagonist activity was investigated with theoretical studies.

It was found that all new *N*,*N*′-diarylureas bind strongly to the active center (primary site) of the enzyme. The strongest binding seems to have compounds **6f**, **6i**, and **11g**. Specifically, compound **6i** forms one hydrogen bond with PHE174 amino acid. Compound **6f** forms two π–π interactions with TRP279 and two hydrogen bonds with PHE117. Compound **11g** forms 5 π–π interactions with TRP279, PHE268, PHE501, and PHE174. Additionally, DFT calculations have shown that these three compounds, **6f**, **6i**, and **11g**, present increased reactivity compared to the remaining studied *N*,*N*′-diarylureas. In all 17 *N*,*N*′-diarylureas present, the H → L excitation is a charge transfer process, while in the cases of the **6f** and **11g**, it is an electron transfer process. MD simulations studied the binding affinity of compounds **6f**, **6i**, and **11g** in the primary site during the time evolution of 200 ns. Regarding the docking of **6f** and **6i**, the protein undergoes significant conformational changes, or there are regions in the protein that are very flexible during the simulation while both **6f** and **6i** remain bound. However, while **6f** maintains its binding orientation, **6i** presents fluctuations. Finally, when **11g** is docked, the protein maintains structural integrity while **11g** undergoes substantial movements or conformational changes within the binding site.

The potential of all new *N*,*N*′-diarylureas to bind in an allosteric position of the CB1 as a complex with the agonist AM841 has been investigated. It was found that all compounds bind to the same pocket, they are located next to the same amino acids, and they bind in an allosteric position. Specifically, 10 out of the 17 compounds studied—that is, **11e, 6d, 6e, 6g, 11d, 6c, 6b, 11b, 6i,** and **6f**—bind stronger than the known inhibitor PSNCBAM-1 or similarly, showing that they have the potential to be used as successfully as allosteric CB-1 receptor inhibitors. The largest binding values are obtained for the compounds **11e**, **6d**, and **6e**. Hydrogen bonds and π–π interactions are formed between the allosteric site position and the compounds. **6d** forms one hydrogen bond with LEU463 and one π–π interaction with HIS304, while compound **6e** forms one hydrogen bond with ARG458 and one π–π interaction with HIS304.

Finally, while in the orthosteric site of the CB1, the binding potential of the compounds follows, in general, the DFT-obtained reactivity trend. On the contrary, in the allosteric site, where the binding is smaller than in orthosteric site, compounds do not follow the DFT reactivity trend. This shows that the molecular structure of the compounds, that is, the substituent group, is more important than the total reactivity trend of the compounds.

Acknowledgements

We appreciate the use of NMR and mass spectrometry facilities funded by the Network of Research Supporting Laboratories of the University of Ioannina.

Conflict of Interest

The authors declare no conflict of interest.

Data Availability Statement

The data that support the findings of this study are available in the supplementary material of this article.

Keywords: cannabinoid receptors · density functional theory · molecular docking · molecular dynamics · pyrazolo-based diaryl ureas · triazolo-based diaryl ureas

[1] A. C. Howlett, L. C. Blume, G. D. Dalton, *Curr. Med. Chem.* **2010**, *17*, 1382.
[2] a) R. Janero, *Expert Opin. Emerging Drugs* **2012**, *17*, 17; b) B. Le Foll, S. R. Goldberg, *J. Pharmacol. Exp. Ther.* **2005**, *312*, 875.
[3] K. Crowley, Kiraga, E. Miszczuk, S. Skiba, J. Banach, U. Latek, M. Mendel, M. Chłopecka, *Int. J. Mol. Sci.* **2024**, *25*, 6682.
[4] T.-T. Wei, M. Chandy, M. Nishiga, A. Zhang, K. Krishna Kumar, D. Thomas, A. Manhas, S. Rhee, J. M. Justesen, I. Y. Chen, H.-T. Wo, S. Khanamiri, J. Y. Yang, F. J. Seidl, N. Z. Burns, C. Liu, N. Sayed, J.-J. Shie, C.-F. Yeh, K.-C. Yang, E. Lau, K. L. Lynch, M. Rivas, B. K. Kobilka, J. C. Wu, *Cell* **2022**, *185*, 1676.
[5] a) R. A. Nouh, A. Kamal, A. Abdelnaser, *Pharmaceutics* **2023**, *15*, 1151; b) M. Mecha, F. J. Carrillo-Salinas, A. Feliú, L. Mestre, C. Guaza, *Front. Cell. Neurosci.* **2020**, *14*, 34.
[6] K. Miranda, P. Mehrpouya-Bahrami, P. S. Nagarkatti, M. Nagarkatti, *Front. Immunol.* **2019**, *10*, 1049.
[7] J. Wang, H.-X. Lu, J. Wang, *J. Pharm. Pharmacol.* **2019**, *71*, 1469.
[8] H. Xu, Y. Chen, H. Tong, L. Chen, C. Morisseau, Z. Zhou, J. Zhuang, C. Song, P. Cai, Z. Liu, B. D. Hammock, G. Chen, *J. Med. Chem.* **2024**, *67*, 12887.
[9] F. Borgan, H. Laurikainen, M. Veronese, T. R. Marques, M. Haaparanta-Solin, O. Solin, T. Dahoun, M. Rogdaki, R. K. R. Salokangas, M. Karukivi, M. Di Forti, F. Turkheimer, J. Hietala, O. Howes, *JAMA Psychiatry* **2019**, *76*, 1074.
[10] F. Borgan, M. Kokkinou, O. Howes, *Biol. Psychiatry Cogn. Neurosci. Neuroimaging* **2021**, *6*, 646.
[11] J. Hirvonen, P. Zanotti-Fregonara, D. A. Gorelick, C. H. Lyoo, D. Rallis-Frutos, C. Morse, S. S. Zoghbi, V. W. Pike, N. D. Volkow, M. A. Huestis, R. B. Innis, *Biol. Psychiatry* **2018**, *84*, 715.
[12] a) D. R. Janero, *Expert Opin. Emerg. Drugs* **2012**, *17*, 17; b) S. J. Ward, R. B. Raffa, *Obesity* **2011**, *19*, 1325.
[13] a) Z. Shao, W. Yan, K. Chapman, K. Ramesh, A. J. Ferrell, J. Yin, X. Wang, Q. Xu, D. M. Rosenbaum, *Nat. Chem. Biol.* **2019**, *15*, 1199; b) J. Yuan, B. Yang, G. Hou, X. Q. Xie, Z. Feng, *Drug Discov. Today* **2023**, *28*, 103615.
[14] a) J. Horswill, U. Bali, S. Shaaban, J. Keily, P. Jeevaratnam, A. Babbs, C. Reynet, P. W. K. In, *Br. J. Pharmacol.* **2007**, *152*, 805; b) T. Nguyen, T. F. Gamage, A. M. Decker, N. German, T. L. Langston, C. E. Farquhar, T. P. Kenakin, J. L. Wiley, B. F. Thomas, Y. Zhang, *ACS Chem. Neurosci.* **2019**, *10*, 518; c) S. Meini, F. Gado, L. A. Stevenson, M. Digiacomo, A. Saba, S. Codini, M. Macchia, R. G. Pertwee, S. Bertini, C. Manera, *Eur. J. Med. Chem.* **2020**, *203*, 112606; d) T. Nguyen, T. F. Gamage, A. M. Decker, D. B. Finlay, T. L. Langston, D. Barrus, M. Glass, D. L. Harris, Y. Zhang, *Bioorg. Med. Chem.* **2021**, *41*, 116215.
[15] a) L. Garuti, M. Roberti, G. Bottegoni, M. Ferraro, *Curr. Med. Chem.* **2016**, *23*, 1528; b) A. Catalano, D. Iacopetta, M. D. Sinicropi, C. Franchini, *Appl. Sci.* **2021**, *11*, 374; c) X. Y. Sun, Z. Z. Xie, X. Y. Lei, S. Huang, G. T. Tang, Z. Wang, *RSC Med. Chem.* **2023**, *14*, 1209.
[16] J. X. Qiao, T. C. Wang, R. Ruel, C. Thibeault, A. L'Heureux, W. A. Schumacher, S. A. Spronk, S. Hiebert, G. Bouthillier, J. Lloyd, Z. Pi, D. Schnur, L. M. Abell, L. A. Price, F. Liu, Q. Wu, T. E. Steinbacher, J. S. Bostwick, M. Chang, J. Zheng, Q. Gao, B. Ma, P. A. McDonnell, C. S. Huang, R. Rehfuss, R. R. Wexler, P. Y. S. Lam, *J. Med. Chem.* **2013**, *56*, 9275.
[17] J. Wua, C. Wanga, D. Leas, M. Vargas, K. L. White, D. M. Sackleford, G. Chen, A. G. Sanford, R. M. Hemsley, P. H. Davis, Y. Dong, S. A. Charman, J. Keiser, J. L. Vennerstrom, *Bioorg. Med. Chem. Lett.* **2018**, *28*, 244.
[18] a) Y. Zhang, M. Anderson, J. L. Weisman, M. Lu, C. J. Choy, V. A. Boyd, J. Price, M. Sigal, J. Clark, M. Connelly, F. Zhu, W. A. Guiguemde, C. Jeffries, L. Yang, A. Lemoff, A. P. Liou, T. R. Webb, J. L. DeRisi, R. K. Guy, *ACS Med. Chem. Lett.* **2010**, *1*, 460; b) J. W. Anderson, D. Sarantakis, J. Terpinski, T. R. Kumar, H. C. Tsai, M. Kuo, A. L. Ager, J. W. R. Jacobs, G. A. Schiehser, S. Ekins, J. C. Sacchettini, D. P. Jacobus, D. A. Fidock, J. S. Freundlich, *Bioorg. Med. Chem. Lett.* **2013**, *23*, 1022.
[19] A. B. Velappan, M. R. C. Raja, D. Datta, Y. T. Tsai, I. Halloum, B. Wan, L. Kremer, H. Gramajo, S. G. Franzblau, S. K. Mahapatra, J. Debnath, *Eur. J. Med. Chem.* **2017**, *125*, 825.
[20] Y. Tsuji, R. Takeuchi, Y. Watanabe, *J. Organomet. Chem.* **1985**, *290*, 249.
[21] X. Wang, P. Li, X. Yuan, S. Lu, *J. Mol. Catal. A: Chem.* **2006**, *255*, 25.
[22] I. Gallou, *Org. Prep. Proced. Int.* **2007**, *39*, 355.
[23] a) H. Q. Zhang, F. H. Gong, J. Q. Ye, C. Zhang, X. H. Yue, C. G. Li, Y. G. Xu, L. P. Sun, *Med. Chem. Commun.* **2013**, *4*, 979; b) H. Gao, P. Su, Y. Shi, X. Shen, Y. Zhang, J. Dong, J. Zhang, *Eur. J. Med. Chem.* **2015**, *90*, 232; c) Y. Shan, C. Wang, L. Zhang, J. Wang, M. Wang, Y. Dong, *Bioorg. Med. Chem.* **2016**, *24*, 750; d) A. G. Sarantou, G. Varvounis, *Molbank* **2023**, *2023*, M1531.
[24] K. J. Padiya, S. Gavade, B. Kardile, M. Tiwari, S. Bajare, M. Mane, V. Gaware, S. Varghese, D. Harel, S. Kurhade, *Org. Lett.* **2012**, *14*, 2814.
[25] S. Kotachi, Y. Tsuji, T. Kondo, Y. Watanabe, *J. Chem. Soc., Chem. Commun.* **1990**, 549.
[26] G. A. Artamkina, A. G. Sergeev, I. P. Beletskaya, *Tetrahedron Lett.* **2001**, *42*, 4381.
[27] R. Hosseinzadeh, Y. Sarrafi, M. Mohadjerani, F. Mohammadpourmir, *Tetrahedron Lett.* **2008**, *49*, 840.
[28] S. N. Gavade, R. S. Balaskar, M. S. Mane, P. N. Pabrekar, M. S. Shingare, D. V. Mane, *Chin. Chem. Lett.* **2011**, *22*, 675.
[29] S. Breitler, N. J. Oldenhuis, B. P. Fors, S. L. Buchwald, *Org. Lett.* **2011**, *13*, 3262.
[30] P. D. Duarte, M. W. Paixão, A. G. Corrêa, *Green Process Synth.* **2013**, *2*, 19.
[31] a) P. Pal, H. P. Gandhi, A.M. K. N.R. Patel, N. N. Mankadia, S. N. Baldha, M. A. Barmade, P. R. Murumkar, M. R. Yadav, *Eur. J. Med. Chem.* **2017**, *130*, 107; b) R. Yamasaki, Y. Honjo, A. Ito, K. Fukuda, I. Okamoto, *Chem. Pharm. Bull.* **2018**, *66*, 880.
[32] a) C. M. G. dos Santos, T. McCabe, G. W. Watson, P. E. Kruger, T. Gunnlaugsson, *J. Org. Chem.* **2008**, *73*, 9235; b) M. W. Holladay, B. T. Campbell, M. W. Rowbottom, Q. Chao, K. G. Sprankle, A. G. Lai, S. Abraham, E. Setti, R. Faraoni, L. Tran, R. C. Armstrong, R. N. Gunawardane, M. F. Gardner, M. D. Cramer, D. Gitnick, M. A. Ator, B. D. Dorsey, B. R. Ruggeri, M. Williams, S. S. Bhagwat, J. James, *Bioorg. Med. Chem. Lett.* **2011**, *21*, 5342; c) Z. Babic, M. Crkvencic, Z. Rajic, A. M. Mikecin, M. Kralj, J. Balzarini, M. Petrova, J. Vanderleyden, B. Zorc, *Molecules* **2012**, *17*, 1124; d) E. J. Koh, M. I. El-Gamal, C. H. Oh, S. H. Lee, T. Sim, G. Kim, H. S. Choi, J. H. Hong, S. Lee, K. H. Yoo, *Eur. J. Med. Chem.* **2013**, *70*, 10; e) J. X. Qiao, T. C. Wang, R. Ruel, C. Thibeault, A. L'Heureux, W. A. Schumacher, S. A. Spronk, S. Hiebert, G. Bouthillier, J. Lloyd, Z. L. Pi, D. M. Schnur, L. M. Abell, J. Hua, L. A. Price, E. Liu, Q. M. Wu, T. E. Steinbacher, J. S. Bostwick, M. Chang, J. N. Zheng, Q. Gao, B. Q. Ma, P. A. McDonnell, C. S. Huang, R. Rehfuss, R. R. Wexler, P. Y. S. Lam, *J. Med. Chem.* **2013**, *56*, 9275; f) Z. Liu, Y. Wang, H. Lin, D. Zuo, L. Wang, Y. Zhao, P. Gong, *Eur. J. Med. Chem.* **2014**, *85*, 215; g) E. Pujol, N. Blanco-Cabra, E. Julián, R. Leiva, E. Torrents, S. Vázquez, *Molecules* **2018**, *23*, 2853.
[33] A. S. Singh, D. Kumar, N. Mishra, V. K. Tiwari, *RSC Adv.* **2016**, *6*, 84512.
[34] A. S. Singh, A. K. Agrahari, S. K. Singh, M. S. Yadav, V. K. Tiwari, *Synthesis* **2019**, *51*, 3443.
[35] S. Chamni, J. Zhang, H. Zou, *Green Chem. Lett. Rev.* **2020**, *13*, 246.
[36] A. Labiche, M. Norlöff, S. Feuillastre, F. Taran, D. Audisio, *Asian J. Org. Chem.* **2023**, *12*, e202200640.
[37] A. K. Ghosh, M. Brindisi, *J. Med. Chem.* **2020**, *63*, 2751.
[38] F. D. Bellamy, *Tetrahedron Lett.* **1984**, *25*, 839.
[39] a) A. D. Becke, *J. Chem. Phys.* **1993**, *98*, 5648; b) C. Lee, W. Yang, R. G. Parr, *Phys. Rev. B* **1988**, *37*, 785.
[40] L. A. Curtiss, M. P. McGrath, J.-P. Blaudeau, N. E. Davis, R. C. Binning Jr, L. Radom, *J. Chem. Phys.* **1995**, *103*, 6104.
[41] S. Miertuš, E. Scrocco, J. Tomasi, *Chem. Phys.* **1981**, *55*, 117.
[42] J. Tirado-Rives, W. L. Jorgensen, *J. Chem. Theory Comput.* **2008**, *4*, 297.
[43] a) D. Tzeli, P. G. Tsoungas, I. D. Petsalakis, P. Kozielewicz, M. Zloh, *Tetrahedron* **2015**, *71*, 359; b) D. Tzeli, I. E. Gerontitis, I. D. Petsalakis, P. G. Tsoungas, G. Varvounis, *ChemPlusChem* **2022**, *87*, e202200313.
[44] J. Tomasi, B. Mennucci, R. Cammi, *Chem. Rev.* **2005**, *105*, 2999.
[45] M. J. Frisch, G. W. Trucks, H. B. Schlegel, G. E. Scuseria, M. A. Robb, J. R. Cheeseman, G. Scalmani, V. Barone, G. A. Petersson, H. Nakatsuji, X. Li, M. Caricato, A. V. Marenich, J. Bloino, B. G. Janesko, R. Gomperts, B. Mennucci, H. P. Hratchian, J. V. Ortiz, A. F. Izmaylov, J. L. Sonnenberg, D. Williams-Young, F. Ding, F. Lipparini, F. Egidi, J. Goings, B. Peng, A. Petrone, T. Henderson, D. Ranasinghe, et al., *Gaussian 16, Revision C.01*, Gaussian, Inc., Wallingford CT **2016**.
[46] F. De Proft, P. Geerlings, *Chem. Rev.* **2001**, *101*, 1451.
[47] R. A. Miranda-Quintana, *Theor. Chem. Acc.* **2017**, *136*, 1.

[48] a) G. Zhang, C. B. Musgrave, *J. Phys. Chem. A* **2007**, *111*, 1554; b) B. K. Ong, K. L. Woon, A. Ariffin, Synthetic Metals **2014**, *195*, 54; c) K. P. Zois, A. A. Danopoulos, D. Tzeli, *ChemPhysChem* **2025**, *26*, e202500012.
[49] T. Hua, K. Vemuri, S. P. Nikas, R. B. Laprairie, Y. Wu, L. Qu, M. Pu, A. Korde, S. Jiang, J. H. Ho, G. W. Han, K. Ding, X. Li, H. Liu, M. A. Hanson, S. Zhao, L. M. Bohn, A. Makriyannis, R. C. Stevens, Z. J. Liu, *Nature* **2017**, *547*, 468.
[50] Schrodinger, L. L. C. MacroModel, Version 10.2. New York **2013**.
[51] W. L. Jorgensen, D. S. Maxwell, J. Tirado-Rives, *J. Am. Chem. Soc.* **1996**, *118*, 11225.

Manuscript received: April 27, 2025
Revised manuscript received: June 13, 2025
Version of record online: